INTERPLANETARY DUST PARTICLES DETECTED BY THE VOYAGER 1 AND 2 PLASMA WAVE INSTRUMENTS

by

Zhenzhen Wang

A thesis submitted in partial fulfillment
of the requirements for the Master of
Science degree in Physics
in the Graduate College of
The University of Iowa

December 2004

Thesis Supervisor: Professor Donald A. Gurnett

Graduate College
The University of Iowa
Iowa City, Iowa

CERTIFICATE OF APPROVAL

_____

MASTER'S THESIS

_____

This is to certify that the Master's thesis of

Zhenzhen Wang

has been approved by the Examining Committee
for the thesis requirement for the Master of Science
degree in Physics at the December 2004 graduation.

Thesis Committee: _____
Donald A. Gurnett, Thesis Supervisor

_____
William Daughton

_____
Kenneth Gayley

ACKNOWLEDGMENTS

First of all I would like to give my sincere gratitude to my advisor, Professor Donald Gurnett, who provided the initial concept for this project. Without his instructions I could not have been able to complete this thesis.

I would also like to thank Ann Persoon, who assisted with the plots and some of the illustrations.

My thanks also go to Kathy Kurth, who helped me format this thesis.

Finally, I would like to thank my parents, who love me and encourage me so much.

ABSTRACT

This thesis describes observations of small dust particles detected in the outer Solar System with the plasma wave instruments on the Voyager 1 and 2 spacecraft. The Voyager 1 and 2 spacecraft were launched separately on September 5 and August 20, 1977, to study the outer planets, Jupiter, Saturn, Uranus, and Neptune, and to study the interplanetary medium. After traveling through space for 27 years, Voyager 1 is now at a radial distance of 94 astronomical units (AU) from the Sun, and Voyager 2 is at 75 AU. During their journeys through the outer Solar System, the plasma wave instruments onboard the two spacecraft have detected a nearly steady rate of impulsive signals in the interplanetary medium (i.e., in regions far from any of the planets). These signals are attributed to small micron-sized particles hitting the spacecraft. When a small particle strikes the spacecraft at a high velocity, the particle is instantly vaporized and heated to a high temperature, producing a cloud of ionized gas that expands away from the impact site. As the ionized gas cloud sweeps over the plasma wave antenna, it causes a voltage pulse, thereby producing the impulsive signals. The impact rate is found to be nearly independent of distance from the Sun and is essentially the same for Voyagers 1 and 2 at an average rate of about 4 to 5 impacts per hour. The time separation between impacts follows a Poisson distribution, which suggests that successive events are uncorrelated. Four possible origins of the dust particles are considered: planets, comets, Kuiper belt objects, and the interstellar medium. Of these, the interstellar medium appears to provide the most likely origin.

TABLE OF CONTENTS

LIST OF TABLES

Table

LIST OF FIGURES

Figure

CHAPTER I

INTRODUCTION

The purpose of this thesis is to study small dust particles detected in the outer Solar System by the plasma wave instruments on the Voyager 1 and 2 spacecraft. Voyager 1, which was launched on September 5, 1977, is now at a heliocentric radial distance of 94 AU (astronomical units), and Voyager 2, which was launched on August 20, 1977, is at 75 AU. During their passage through the Solar System, the plasma wave instruments on both spacecraft have detected a nearly constant level of impulsive signals in the interplanetary medium at a rate of about several per hour. The impulsive signals can not be due to locally generated plasma waves because the spectrum of these signals extends well above the local electron plasma frequency, which is the highest frequency that can be expected for a locally generated plasma wave, and are believed to be produced by small micron-sized dust particles hitting the spacecraft.

The theory of how these dust particles produce impulsive signals in the plasma wave data is complicated. In the vast space of the outer Solar System, it is thought that there are many very small dust particles. Because of the very large velocity of the spacecraft (about 14 km/second relative to the Sun), when the spacecraft hits one of these particles the particle is instantly vaporized, thereby producing a small partially ionized cloud of gas called a plasma that rapidly expands outward from the point of impact. Some of the charge in this cloud is subsequently collected by the plasma wave electric field antenna, thereby producing an impulsive signal in the electric field waveform (Gurnett et al., 1982).

At the present time there are very few measurements of dust particles in the outer Solar System, and none at the very large heliocentric radial distance where the Voyager measurements are being obtained. Only three other spacecraft, Ulysses,

Galileo, and Cassini, have instruments (called micrometeoroid detectors) capable of detecting small dust particles in the outer Solar System. The Ulysses and Galileo measurements are all restricted to the region near and inside the orbit of Jupiter, which is at 5.2 AU, and the Cassini measurements are restricted to the region near and inside the orbit of Saturn, which is at 9.6 AU. For a summary of results from the micrometeoroid detectors on the Galileo and Ulysses spacecraft, see Grun et al. (1993). Grun's early results suggested that comets and asteroids were the primary sources of small dust particles in the inner region of the Solar System. However, when the Ulysses spacecraft flew by Jupiter in 1992, the micrometeoroid detector recorded periodic bursts of sub-micrometer-sized dust particles arriving in collimated streams from the line-of-sight direction to Jupiter. These observations demonstrated that planets such as Jupiter are significant sources of interplanetary dust. Also, Ulysses detected a flux of micrometer-sized dust particles moving in high-velocity ($\geq$26 km/second) retrograde orbits (Grun et al., 1993). Those dust particles were subsequently identified as being of interstellar origin. As the Galileo spacecraft traversed interplanetary space between Earth and Jupiter from January 1993 to December 1995, a relatively constant impact rate of interplanetary and interstellar particles was detected at rates of about 0.4 impacts per day over the entire three-year time span. In the outer Solar System (outside about 2.6 AU) the particles are mostly of interstellar origin, whereas in the inner Solar System (inside of 2.6 AU) the particles are mostly of Solar System origin. Within about 1.7 AU from Jupiter, intense streams of small dust particles were detected by the Galileo micrometeoroid detector with impact rates of up to 20,000 per day with impact directions compatible with a Jovian origin (Kruger et al., 1998).

This study of interplanetary dust particles will be carried out as follows. First, we will describe the Voyagers' mission and the plasma wave investigation. This will include a description of the trajectories of Voyagers 1 and 2 and the details of the

plasma wave instruments. Second, we will provide the background and mechanism of dust detection by the plasma wave instruments. Third, we will provide a detailed description of the data observed and the results of the analysis, including impact rates and the distribution of time separations between impacts. Fourth, we will investigate possible sources of the interplanetary dust particles. Four possible sources will be considered: planetary, comets, Kuiper belt objects, and the interstellar medium. Finally, we will give our interpretation and conclusions.

CHAPTER II

DESCRIPTION OF THE INSTRUMENTATION

In the following, we give an overview of the Voyager 1 and 2 spacecraft and their trajectories and describe the plasma wave instrument.

2.1. The Voyager Spacecraft and Their Trajectories

The Voyager 1 and 2 spacecraft were launched separately on September 5 and August 20, 1977. The mission of the Voyager spacecraft was to explore the outer planets, Jupiter, Saturn, Uranus, and Neptune, and to study the interplanetary medium. During their long journeys, they carried out flybys of the giant outer planets and now are traveling outward toward interstellar space at radial velocities of about 3.5 AU per year. Voyager 1 is now (November 2004) at a radial distance of 94 AU from the Sun, and Voyager 2 is at 75 AU. Figure 1 shows a sketch of the Voyager spacecraft. Two cylindrical antenna elements are included on each spacecraft for detecting radio and plasma waves. The plasma wave instrument detects the differential voltage between the two elements, so that the antenna operates as a dipole. Figure 2 shows the trajectories of Voyagers 1 and 2 with some of the most important events indicated. Voyager 1 made its closest approach to Jupiter on March 5, 1979, and then flew by Saturn on November 12, 1980. During the Saturn flyby, the spacecraft was deflected northward out of the ecliptic plane and then headed outward toward interstellar space. Voyager 2 made its closest approach to Jupiter on July 9, 1979, and flew by Saturn on August 25, 1981. It subsequently flew by Uranus on January 24, 1986, and by Neptune on August 25, 1989. During the Neptune flyby, the spacecraft was deflected southward out of the ecliptic plane and then headed outward toward interstellar space.

2.2. Description of the Voyager Plasma Wave Instrument

The Voyager plasma wave system is composed of two antenna elements, which are used as a dipole electric field antenna, and the main electronics package (Scarf and Gurnett, 1977). The antenna elements are each 10 meters long and 1.3 cm in diameter, and are mounted in a V configuration as shown in Figure 1.

All of the signal processing for the plasma wave system is performed in the main electronics box. A block diagram of the electronics in the main electronics package is shown in Figure 3, and a summary of the basic instrument characteristics is given in Table 1. The main electronics package is composed of six elements: two preamplifiers, a switchable attenuator, a differential amplifier, a notch filter, a 16-channel spectrum analyzer, and a wideband receiver. The function of each of these elements is described below.

2.2.1. Preamplifiers

There are two pairs of preamplifiers in the electronics package. The preamplifiers are connected to the antennas and amplify the signals collected by the antennas. One pair of them is connected directly to the antennas ($\times 1$), and the other pair has 40 dB attenuators between the antennas and the preamplifiers ($\times 0.01$). Usually, in dust detection, we only use the former pair.

2.2.2. Switchable Attenuator

If unusually large signals are detected, a switchable attenuator can be commanded to shift the dynamic range toward higher amplitudes, thereby avoiding saturation in the subsequent instrumentation. This attenuator is normally switched off, as saturation has never been a problem.

2.2.3. Differential Amplifier

The differential amplifier is used to provide a dipole response from the two antenna elements. It provides an output signal that is proportional to the voltage difference between the antenna elements.

2.2.4. Notch Filter

The notch filter is used to attenuate interference signals at the spacecraft power supply frequency, 2.4 kHz, and its third harmonic, 7.2 kHz.

2.2.5. 16-Channel Spectrum Analyzer

The 16-channel spectrum analyzer consists of 16 discrete filters logarithmically spaced from 10 Hz to 56.2 kHz and provides low-time-resolution electric field spectrums. The outputs from these filters are switched into two logarithmic detectors which provide an output voltage (0 to 3V) to the spacecraft data system. The spectrum analyzer system gives absolute electric field spectral densities, but with relatively low time resolution, normally one spectrum every 4 seconds.

2.2.6. Wideband Waveform Receiver

The waveform amplifier and associated A/D converter shown in Figure 3 provide the data we use most often in the analysis of dust impacts. They provide very high-time-resolution voltage waveforms from the electric field antenna. A bandpass filter ahead of the waveform amplifier limits the bandwidth of the wideband receiver to the range from 50 Hz to 10 kHz. There is an automatic gain control in the waveform amplifier. The automatic gain control is used to maintain an essentially constant long term root-mean-square output from the amplifier. The time constant of the automatic gain control feedback loop is 0.5 sec. The output of the waveform amplifier is sampled at a rate of 28,800 samples per second by a 4-bit A/D converter. These measurements can be either recorded by the spacecraft data storage system, or transmitted to the ground in real-time. The waveform channel provides an enormous increase in our

ability to identify and analyze wave phenomena because the wideband measurement gives virtually continuous waveform coverage in frequency and time, subject only to the constraints of the uncertainty theorem $\Delta f \, \Delta t \geq 1$.

CHAPTER III

PHYSICS OF DUST IMPACTS

In this chapter, we provide the physics background involved in the detection of dust impacts. We will discuss how dust impacts were detected the first time and the physical mechanism involved in dust detection.

3.1. Description of the First Observation at Saturn

In 1982, a region of very strong intense impulsive noise was detected by the Voyager 2 plasma wave instrument as the spacecraft flew through the ring plane at Saturn (Gurnett et al., 1982). Because of the impulsive nature of the signals and the fact that their spectra extended well above the local electron plasma frequency, it was concluded that the signals were produced by impacts of small dust particles associated with Saturn's rings. This was the first time that dust impacts were detected by a plasma wave instrument. Detailed analyses showed that the particles had radii in the range from about 0.3 to 3 μm. The maximum impact rate at the ring plane crossing was determined to be several hundred impacts per second, and the effective north-south thickness of the particle impact region was found to be 106 km (Gurnett et al., 1983).

3.2. The Dust Impact Ionization Mechanism

The dust particles we discuss here are very small, with masses in the range from about 10^{-15} to 10^{-11} grams. To be detected by the plasma wave instrument, the dust particles must generate an electrical signal that can be detected by the electric field antenna. To understand how the impacts are detected, we need to explain the mechanism that converts the mechanical energy of a dust impact into an electrical signal. Although various mechanisms exist for converting the impact energy to an electrical signal, impact ionization is believed to be the dominant mechanism.

When a high-velocity particle, traveling at speeds of many kilometers per second, strikes a solid object, the kinetic energy is converted into heat which vaporizes both the particle and part of the target material, thereby producing a small partially ionized cloud of gas (Gurnett et al., 1983). After a very short time in which collisions dominate, the gas stops recombination and expands as a cloud of fully ionized plasma. The expansion of the plasma cloud is controlled by the self-consistent electric and magnetic field forces present in the plasma. Because of the pressure imbalance, the plasma cloud rapidly expands outward from the point of impact, as illustrated in Figure 4. The amount of charge released by such a high velocity impact has been studied in the laboratory by several investigators (Friichtenicht, 1964; Auer and Sitte, 1968; Adams and Smith, 1971; Dietzel et al., 1973; McDonnell, 1978; Grun, 1981). These experiments show that the charge Q released in the impact is directly proportional to the mass m of the projectile,

$$Q = km \tag{1}$$

where k is a constant that depends on the speed of the projectile and the composition of the projectile and the target (Grun,1981).

Let us consider a specific example. We will assume that a dust particle (water ice) has a relative speed between the particle and the spacecraft of 13.8 km/sec, which is the approximate velocity of the spacecraft relative to a dust particle at rest. For a dielectric particle such as water ice striking a metal surface such as aluminum, at a speed of 13.8 km/sec the conversion constant, k, is 0.21C/g. If the dust particle has a radius of r = 10 μm and density ρ = 0.92 gcm^{-2} (water ice), then the charge produced by impact is about Q = 8.1×10^{-10}C. If all of this charge (of one sign) were to be collected by the antenna, the resulting antenna voltage would be

$$V = Q / C_A = 9 \text{ V}. \quad (2)$$

This is a large enough voltage to easily explain the observed signal level (10^{-3} - 10^{-1} V) even if only a small part of the charge is collected or if the particles are much smaller than given in this example.

Another possible mechanism was also mentioned in Gurnett et al. (1983). It considered the possibility that the antenna was directly detecting the charge of the dust particle that hits the spacecraft. But they found that for this situation, for a particle of $10\mu m$ in radius, the charge works out to be only $Q = 1.1 \times 10^{-14}$ C. If such a particle hits one of the antennas, the voltage produced is just

$$V = Q / C_A = 1.2 \times 10^{-4} \text{ V} \quad (3)$$

which can be neglected compared with the charge released via the impact ionization effect.

Although we know the linear relationship between the mass of the dust particle and the voltage detected, because of the lack of knowledge of the impact position on the spacecraft and the complex geometry of the spacecraft body, it is difficult for us to derive exact mass and size distributions of the impacting dust particles.

CHAPTER IV

OBSERVATIONS

As we described previously, the voltage waveforms used to detect dust impacts were obtained from the wideband receiver. Generally, the dust impact waveforms consist of an abrupt step rising at near the time resolution of the wideband channel, which is about 30 μsec, followed by a transient recovery lasting from one half to several msec. Both positive and negative pulses occur with about the same frequency, consistent with the fact that the signals detected by the two antennas are of opposite polarity because of the differential response.

An example of a wideband antenna voltage waveform that shows an impulsive dust impact detected by Voyager 2 is shown in Figure 5. This impact occurred at 15:41:59 UT, on day 357, 1997, at a heliocentric radial distance of R = 53.62 AU. From this figure, we can see that the antenna voltage dropped rapidly in a time period of about 0.2 msec, and then experienced a very quick recovery which lasted only about 0.3 msec before recovering back to the equilibrium level.

A summary of all such dust impacts detected by Voyagers 1 and 2 in the interplanetary medium is given in Table 2. Since we want to concentrate on the detection of dust particles in the interplanetary medium, we have eliminated all observations within 500 planetary radii of a planet. The first column gives the radial distance range in which the observations were obtained. The second column gives the range of ecliptic latitudes in which the observations were obtained. The third column gives the number of impacts detected. Due to the limited data storage space in the spacecraft data system, usually only one 48-sec data frame is collected each week. The fourth column gives the number of 48-sec data frames analyzed in each radial distance range. The fifth column gives the number of seconds of data analyzed. The sixth

column gives the duty cycle, which is defined as the ratio of the number of seconds of data analyzed to the total time. The last (seventh) column gives the impact rate, which is the ratio of the number of impacts detected to the number of seconds of data analyzed. For instance, for Voyager 1, 7 impacts were detected in the radial distance range from 45 to 55 AU for ecliptic latitudes in the range from 33.17^{o} to 33.76^{o}. The average impact rate in this radial distance range was 4.02 impacts per hour.

Using the data in Table 2 a plot of the dust impact rate detected by Voyager 1 has been produced as a function of heliocentric radial distance and is shown in Figure 6. The horizontal axis gives the radial distance from the Sun in units of AU, and the vertical axis indicates the impact rate. The vertical lines with short horizontal bars at both ends give the statistical uncertainty in the impact rate. The impact rate starts at 2.75 impacts per hour at 10 AU and has a maximum of 9.92 impacts per hour at a distance of 80 AU. The average impact rate over the entire range for which measurements are available, from 5 to 94 AU, is 3.9 impacts per hour. Although there are variations in the measured impact rate from one radial distance bin to another, the data points are consistent to within statistical accuracy to a constant impact rate, independent of radial distance of about 4 impacts per hour.

Due to technical problems, Voyager 2 stopped transmitting information on dust impacts at a distance of around 65 AU from the Sun. A plot of the impact rate detected by Voyager 2 is shown in Figure 7 as a function of radial distance from 5 to 65 AU. Again the impact rate is statistically indistinguishable from a constant rate independent of radial distance. The average impact rate over the range shown is 4.8 impacts per hour, only slightly larger than the comparable value for Voyager 1. Since Voyagers 1 and 2 left the ecliptic plane at quite different ecliptic latitudes, the close similarity of the dust impact rates at Voyagers 1 and 2 shows that the dust distribution is essentially independent of ecliptic latitude. The radically different trajectories of Voyagers 1 and 2

relative to the ecliptic plane are shown in Figure 8, along with the locations of each dust impact.

CHAPTER V

ANALYSIS AND INTERPRETATION

The question of the origin of those dust particles is intriguing. As mentioned before, there are four possible sources: planets, comet dust trails, the Kuiper belt, and the interstellar medium. We will analyze them one by one according to their respective characteristics.

5.1. Planetary Sources

Possible planetary sources include the nine planets of our Solar System, their moons, and the unique systems of rings. In chapter four, we emphasized that for our project we have considered only the dust impacts that occurred at large distances from the planets. The term "distance" here means at least 500 times the planet's radius when the Voyagers passed near a planet. Under this limited condition, we can rule out planetary sources. The reason is that particles from planetary sources are in general gravitation bound to the near vicinity of the planet and would be excluded by our selection criterion. There are only rare possibilities for such particles to escape and wander into the region where the impacts reported in this study are detected. Since the impact rate remains essentially constant well beyond the orbit of Pluto with no tendency to decrease with increasing radial distance, it is clear that the dust impacts detected by the Voyagers in our study are not due to planetary sources.

5.2. Comet Dust Trails

It is well known that comets produce dust in a long, well-defined trail that is affected by photons emitted from the Sun. Typically this trail curves slightly due to the comet's motion. The trail fades as the comet moves far from the Sun. Refer to Figure 9. From this description, we can see that if the Voyagers encountered a comet dust trail, because of the much higher density of dust particles in the trail, there should be a burst

of many impacts in a short period of time separated by long periods during which no impacts are observed. But we did not observe this situation, and comet dust trails are thought to be an unlikely source of the interplanetary dust impacts detected by Voyagers.

5.3. Kuiper Belt Objects

The Kuiper belt is a region beyond the planet Neptune in which at least 70,000 small, icy, slow-moving objects orbit. These relatively dark objects, called "trans-Neptunians," are perhaps from 10-50 km in diameter. This belt is located from roughly 30 to over 50 AU from the Sun. It was discovered in 1992 by Luu and Jewitt (1996).

Figure 10 shows the inclination distribution of the Kuiper belt objects. It shows that most of the objects, about 90%, were found at inclinations lower than 10 degrees (Brown, 2001). So most of the Kuiper belt objects orbit around the Sun in a plane quite close to the ecliptic plane. If we suppose the Kuiper belt objects are the origin of dust particles, judging from this inclination distribution graph, the impact rates before the Voyager 2 spacecraft flew by Neptune should be much larger than those measured after Voyager 2 flew southward below the ecliptic plane. In fact, the impact rate does not show this variation. So, we rule out the Kuiper belt objects.

5.4. Interstellar Medium

Finally, let us consider the interstellar medium. It is necessary here to mention the paper “Discovery of Jovian dust streams and interstellar grains by the Ulysses spacecraft” (Grun et al., 1993). In this paper, they identified a flux of micrometer-sized dust particles as being of interstellar origin. They give the mass flux of the particles as 6×10^{-17}g m^{-2}s^{-1}, and the mean particle mass as 8×10^{-13} g . So we can derive the number flux.

$$\text{The number flux} = \frac{\text{mass flux}}{\text{mean mass}} \tag{4}$$

$$= 0.75 \times 10^{-4}\ \text{m}^{-2}\ \text{s}^{-1}\ .$$

Now, let us calculate our number flux. The impact rate is 3 per hour and the effective areas of the spacecraft are $A_s = 1.66 \times 10^4\ \text{cm}^2$. Thus

$$\text{The number flux} = \frac{\text{impact rate}}{\text{effective areas of spacecraft}} \tag{5}$$

$$= 0.5 \times 10^{-3}\ \text{m}^{-2}\ \text{s}^{-1}\ .$$

The two results are close, less than order of magnitude, and this provides strong evidence supporting an interstellar origin.

One of the characteristics of the interstellar particles coming into the Solar System is that they should be totally random. The distribution of the intervals between impacts should fit a Poisson distribution function $N_m = N_0 e^{-\gamma \Delta t}$ if the impacts are produced by dust particles originating from the interstellar medium. This is in strong contrast to cometary dust streams, which would be expected to occur in well-defined episodes with many impacts separated by intervals in which very few impacts are observed. We find that the distribution of the intervals between impacts provides a good fit to a Poisson distribution. We also find the best-fit curves by finding the minimum of the standard deviation. Figure 11, 12 and 13 are graphs indicating the distribution of the intervals between events. Figure 11 is for Voyager 2. We combined the data of both spacecraft and obtained Figure 12 and Figure 13 (only data after 1986). The horizontal axis, x, shows the time between events in units of 25 days, and the vertical

axis, y, represents the number of events in each interval along the x axis. These distributions provide a good fit to a Poisson function, especially in Figure 12 and Figure 13, which have better data coverage. This result indicates that the impact events occurred totally randomly.

For the above reasons, we conclude that the dust particles detected by the Voyager spacecraft while traveling through the outer Solar System can originate from the interstellar medium.

Table 1

Voyager Plasma Wave Instrument Characteristics

Measurement Performed	
Electric field components of plasma waves are measured over the frequency range from 10 Hz to 56.2 kHz with the sensitivity of $0.3\mu m^{-1}$ and a dynamic range of 140 dB.	
Instrument Technique	
Spectrum analyzer	16 frequency channels, four channels per decade, bandwidth ~15%, sampled one channel at a time, minimum time between samples 0.5 sec, 8-bit resolution.
Waveform amplifier	Automatic gain control amplifier, sampled 28,800 sec^{-1} with 4-bit resolution (115,200 bps), recorded using the spacecraft data storage system for selected periods during encounter.
Main Instrument Box	
Mass	1.4 kg
Power	Waveform off: -1.1 W Waveform on: -1.6 W
Size	31.8 cm x 18.5 cm x 4.8 cm
Thermal	Thermal blanket required, normal operating range -20^{o} C to $+75^{o}$C.
Telemetry	Spectrum analyzer, 32 bps nominal at encounter. Waveform amplifier, 115.2 kbs, recorded at selected times during encounter.
Commands	One bi-level command for input range control and one bi-level command for turning the waveform power on and off.
Electric Field Antenna	
Length	Two 10m elements, used as a balanced dipole, with 7m effective length.

Table 2

Summary of Dust Impacts Detected by Voyagers 1 and 2
and Available Data Coverage

Radial Distance (AU)	Ecliptic Latitude (degrees)	Number of Impacts Detected	Number of 48-sec Frames Analyzed	Number of Seconds Analyzed	Duty Cycle ($\times 10^{-5}$)	R Impact Rate Per Hour
			Voyager 1			
5-15	0.63 - 22.06	6	193	7842.25	7.89	2.75
15-25	22.06 - 29.73	8	134	5794.89	6.34	4.97
25-35	29.73 - 32.10	3	110	4768.84	5.46	2.26
35-45	32.10 - 33.17	6	120	5191.61	5.98	4.16
45-55	33.17 - 33.76	7	236	6261.72	7.21	4.02
55-65	33.76 - 34.13	0	149	1284.27	1.48	0.00
65-75	34.13 - 34.38	1	146	1240.10	1.42	2.90
75-85	34.38 - 34.56	6	333	2796.31	3.20	7.72
85-95	34.56 - 34.69	2	183	1474.15	2.49	4.88
			Voyager 2			
5-15	1.14 - 0.46	11	280	12071.90	8.15	3.28
15-25	0.46 - 0.58	24	323	13476.50	12.58	6.41
25-35	0.58 - -6.95	21	351	13184.60	12.07	5.73
35-45	-6.95 - -16.89	11	329	14294.00	12.75	2.52
45-55	-16.89 - -22.83	10	178	7462.93	7.07	5.31
55-65	-22.83 - -26.82	3	170	1954.15	1.91	5.53
65-75	-26.82 - -29.70	0		0.00		0.00
75-85	-29.70 - -31.87	0		0.00		0.00

Figure 1. A sketch of the Voyager spacecraft showing the mounting of the two antenna elements. The plasma wave instrument detects the differential voltage between the two antenna elements.

C-D82-478-12

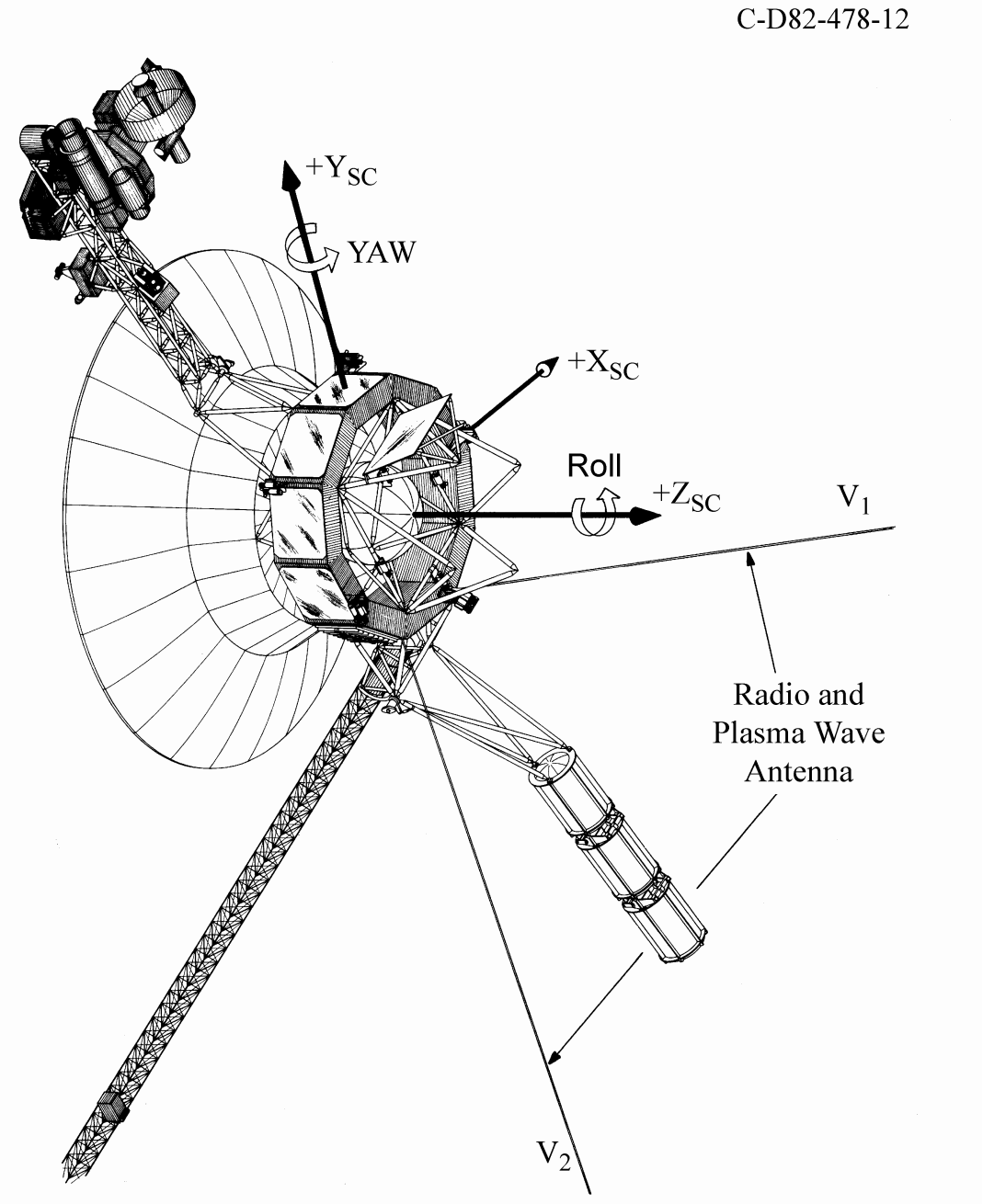

Figure 2. The trajectories of Voyager 1 and Voyager 2 with a few important events indicated.

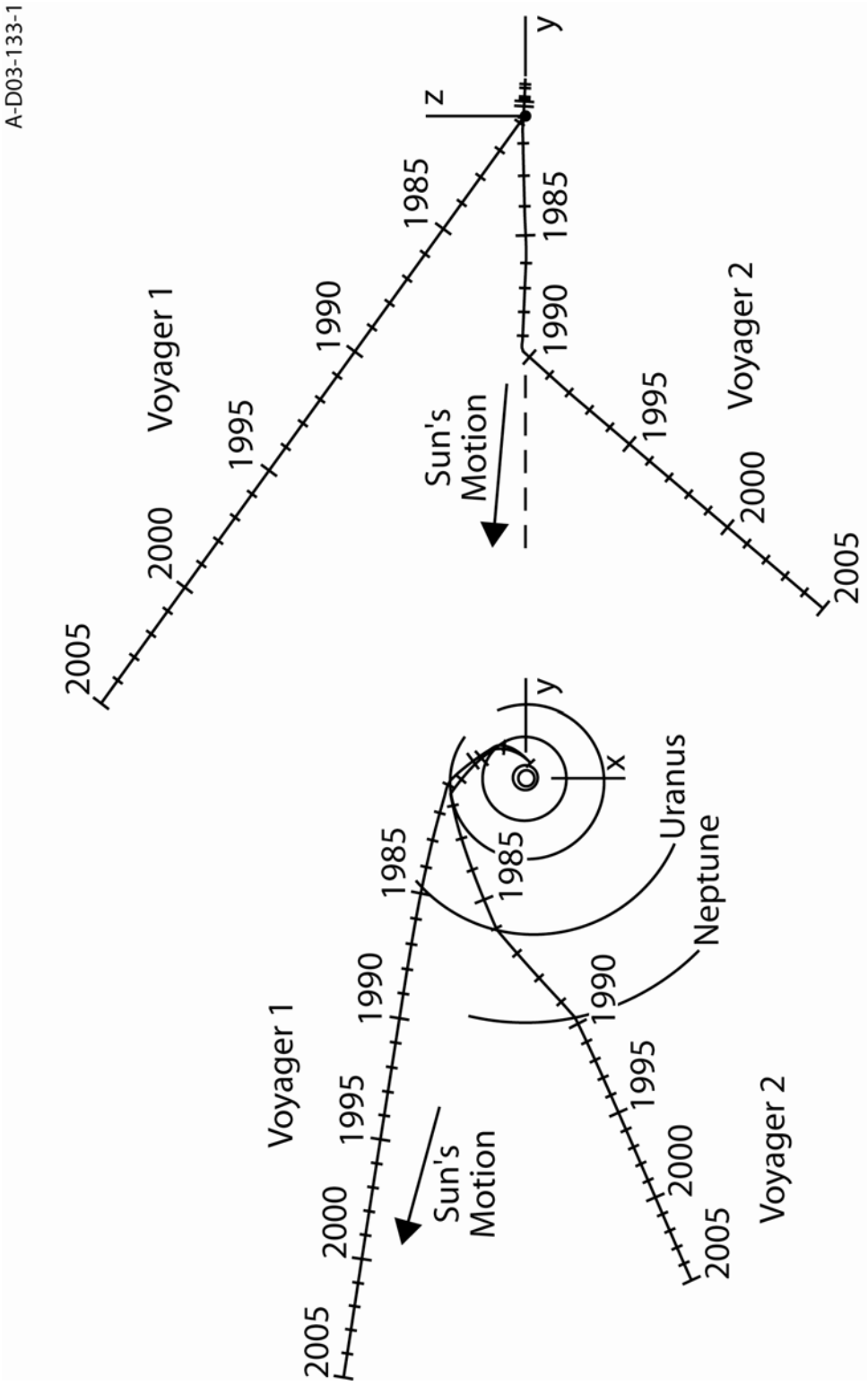
A-D03-133-1
Voyager 1
2005
2000
1995
1990
1985
Sun's
Motion
z
y
1985
1990
1995
2000
2005
Voyager 2
Voyager 1
2005
2000
1995
1990
1985
Sun's
Motion
y
x
1985
Uranus
Neptune
1990
1995
2000
2005
Voyager 2

Figure 3. The Voyager Plasma Wave Subsystem block diagram.

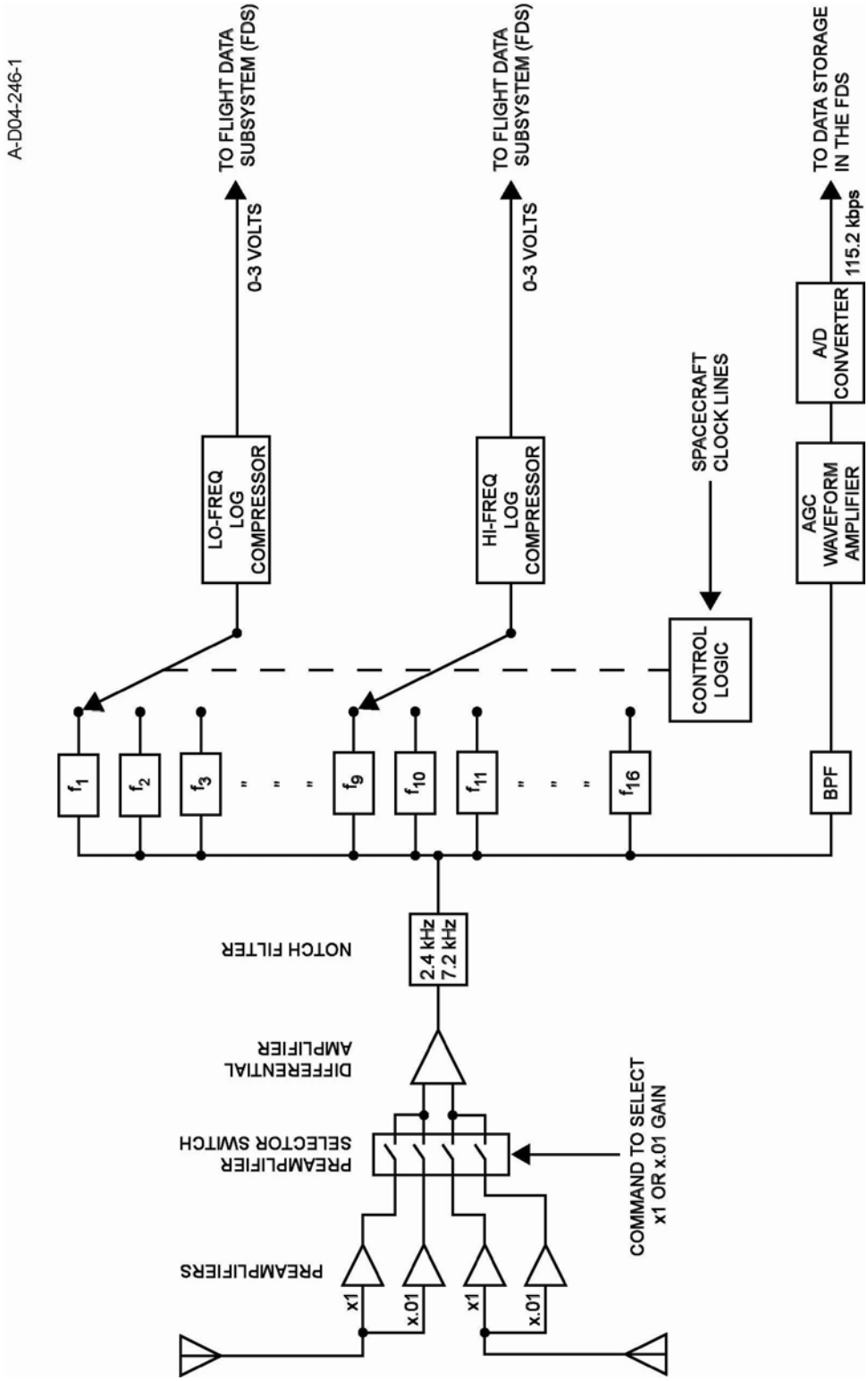
A-D04-246-1
TO FLIGHT DATA SUBSYSTEM (FDS)
0-3 VOLTS
LO-FREQ LOG COMPRESSOR
TO FLIGHT DATA SUBSYSTEM (FDS)
0-3 VOLTS
HI-FREQ LOG COMPRESSOR
SPACECRAFT CLOCK LINES
CONTROL LOGIC
TO DATA STORAGE IN THE FDS
115.2 kbps
A/D CONVERTER
AGC WAVEFORM AMPLIFIER
BPF
f1
f2
f3
f9
f10
f11
f16
NOTCH FILTER
2.4 kHz
7.2 kHz
DIFFERENTIAL AMPLIFIER
PREAMPLIFIER SELECTOR SWITCH
COMMAND TO SELECT x1 OR x.01 GAIN
PREAMPLIFIERS
x1
x.01
x1
x.01

Figure 4. An illustration of the plasma cloud produced by impact ionization. The antenna voltage is $V = Q / C_A$, where Q is the charge collected by one of the antenna elements and C_A is the capacitance of the antenna.

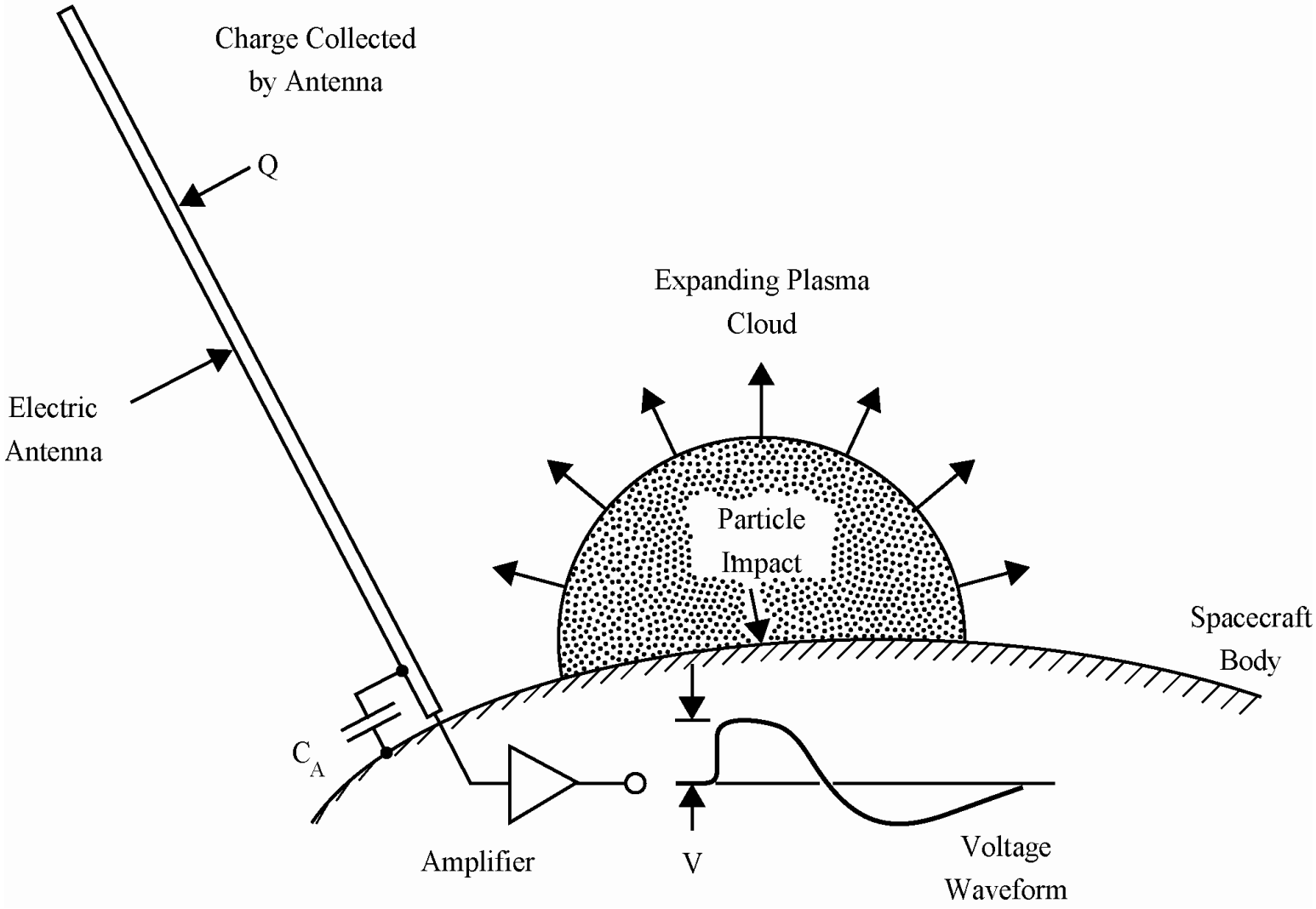
Charge Collected
by Antenna
Q
Expanding Plasma
Cloud
Electric
Antenna
Particle
Impact
Spacecraft
Body
C_A
Amplifier
V
Voltage
Waveform

Figure 5. A diagram showing the wideband waveform of an impulsive event detected by Voyager 2 on day 357, 1997 at 15:41:59 UT, R=53.62 AU. Dust impacts have the characteristics on the wave form of falling rapidly in a very small time period and then recovering very quickly.

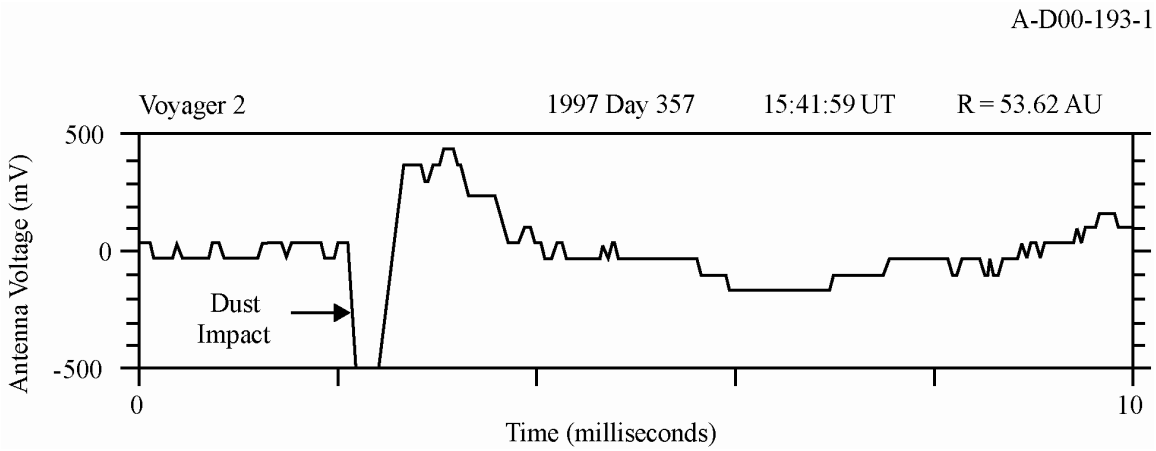
A-D00-193-1
Voyager 2
1997 Day 357
15:41:59 UT
R = 53.62 AU
500
0
-500
Antenna Voltage (mV)
Dust
Impact
0
10
Time (milliseconds)

Figure 6. An illustration showing the impact rate detected by Voyager 1 versus the distance from the Sun for Voyager 1. The impact rate distributes randomly and the bars indicate standard deviation.

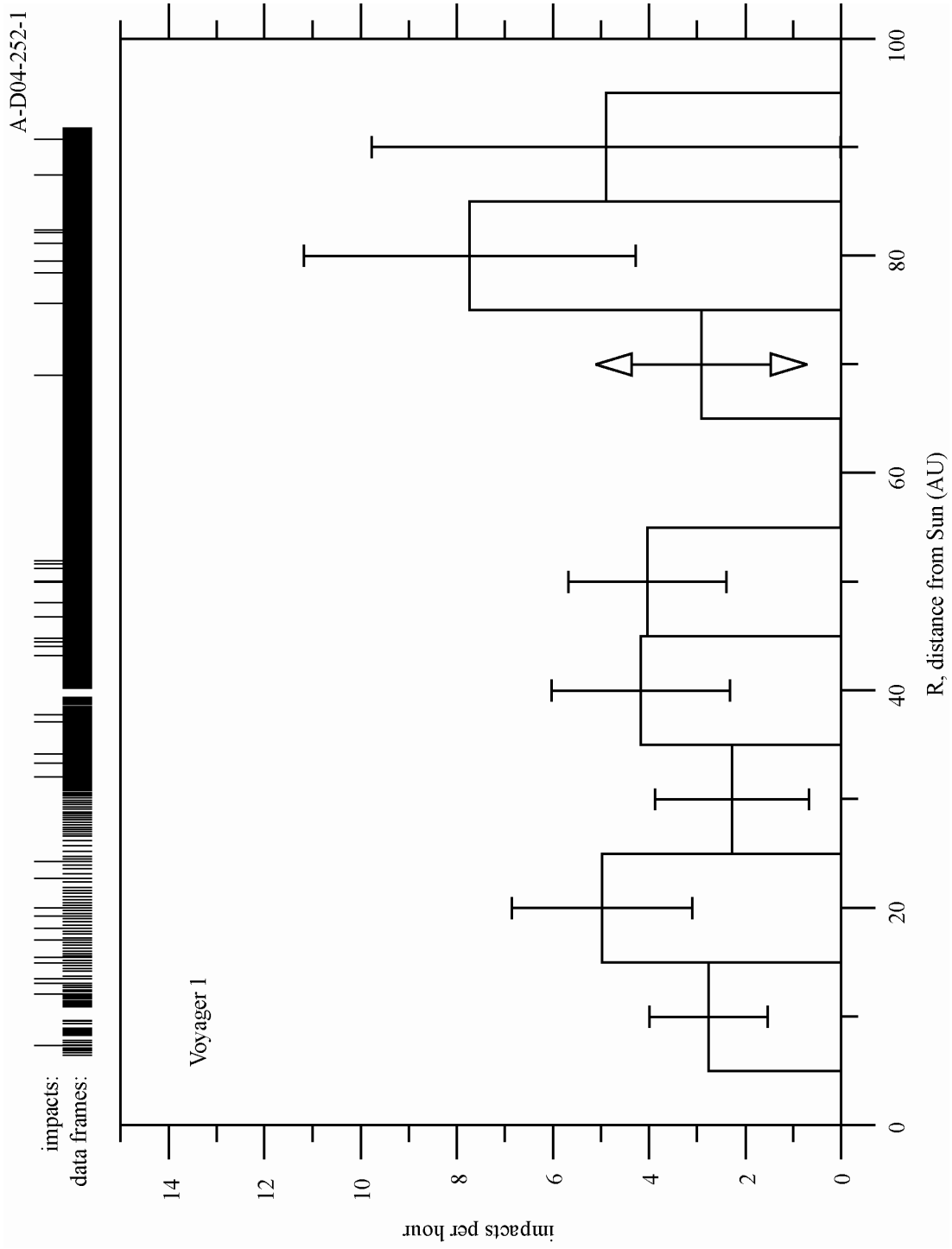
A-D04-252-1
impacts:
data frames:
Voyager 1
impacts per hour
0
2
4
6
8
10
12
14
0
20
40
60
80
100
R, distance from Sun (AU)

Figure 7. An illustration showing the impact rate detected by Voyager 2 versus the distance from the Sun for Voyager 2. The impact rate distributes randomly and the bars indicate standard deviation.

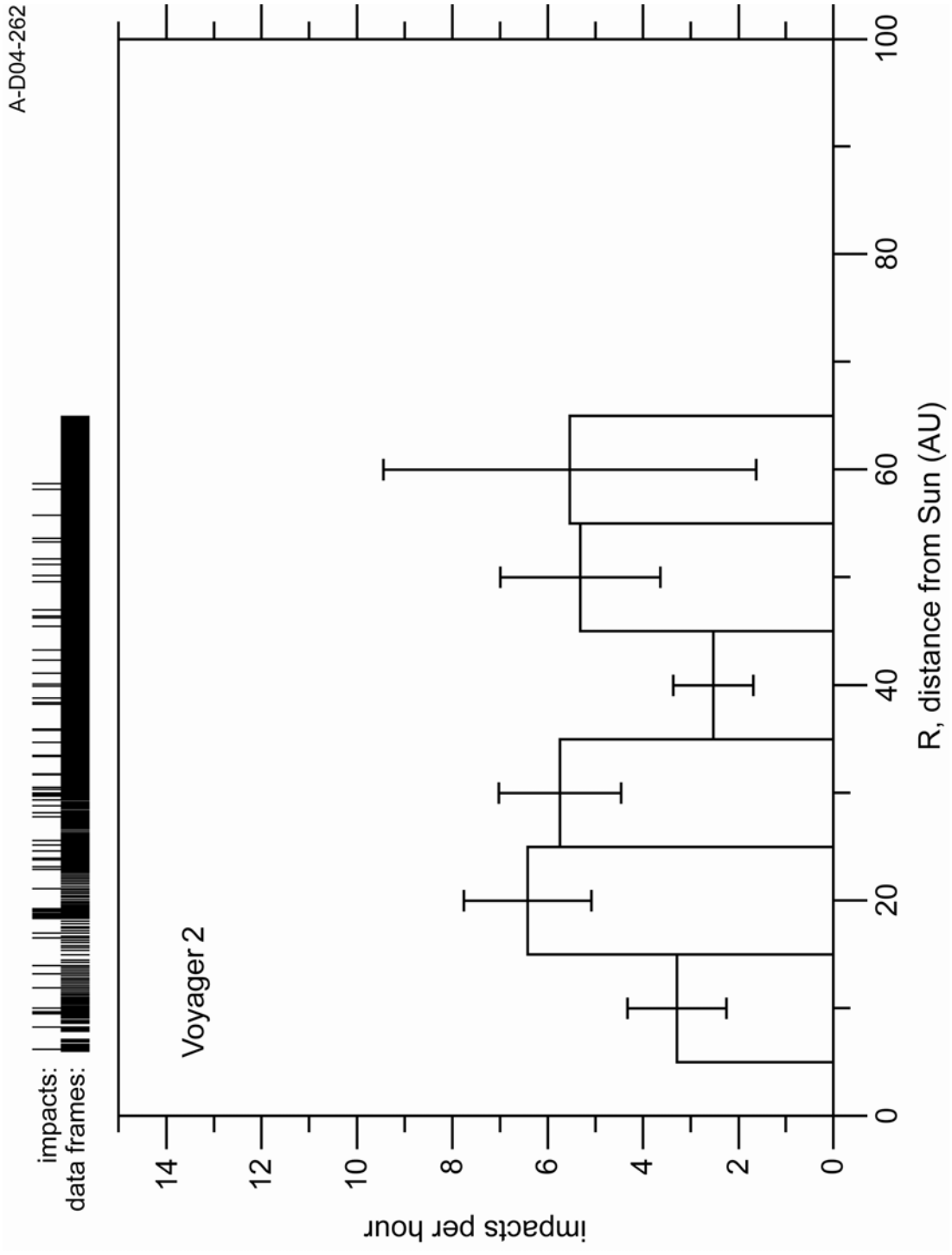
A-D04-262
impacts:
data frames:
Voyager 2
impacts per hour
0
2
4
6
8
10
12
14
0
20
40
60
80
100
R, distance from Sun (AU)

Figure 8. Two-dimensional sketch showing the distance between the Voyagers and the Sun projected on the ecliptic plane. The vertical axis shows the distance above ecliptic plane.

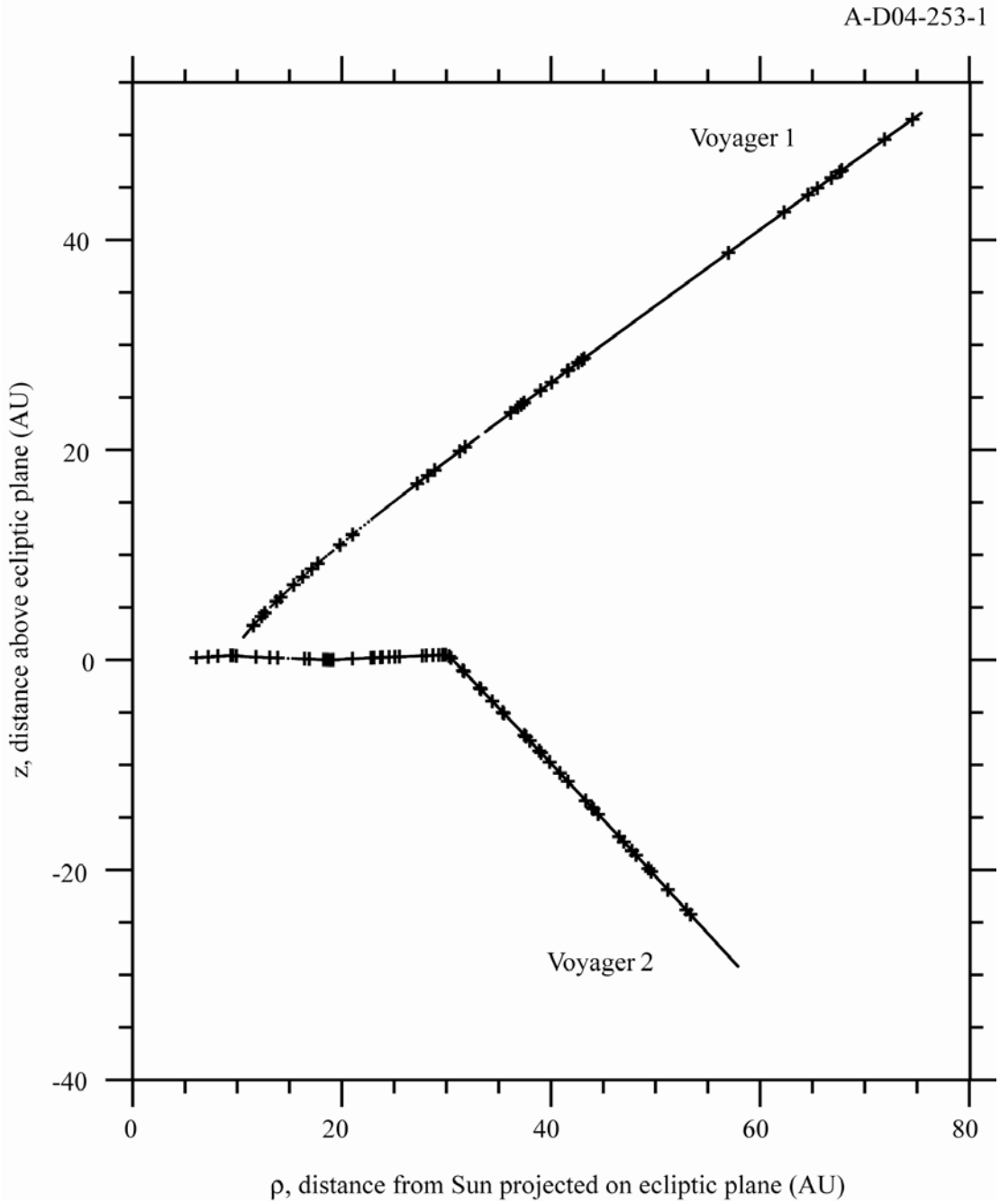
A-D04-253-1
Voyager 1
Voyager 2
40
20
0
-20
-40
0
20
40
60
80
z, distance above ecliptic plane (AU)
ρ, distance from Sun projected on ecliptic plane (AU)

Figure 9. A schematic illustration of a comet dust trail.

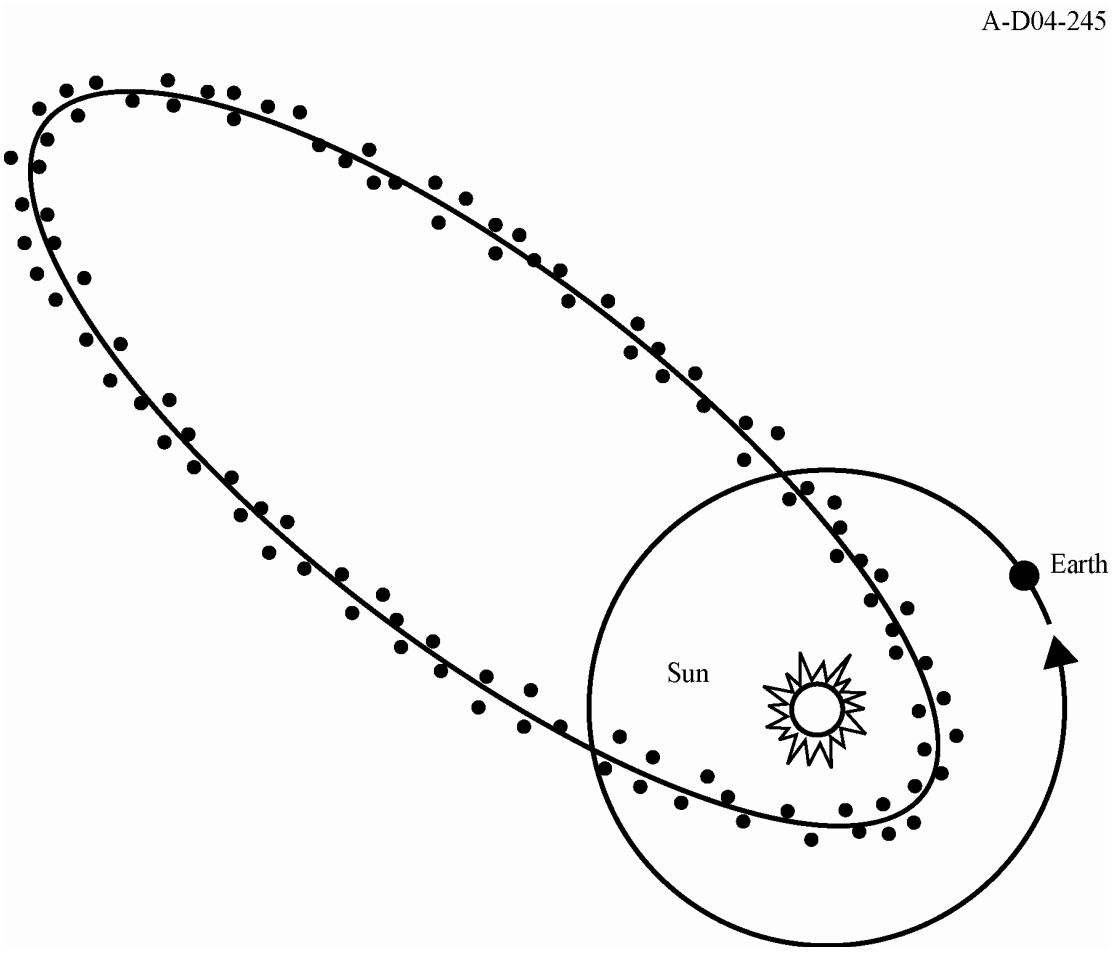
A-D04-245
Earth
Sun

Figure 10. An illustration showing the inclination distribution of the Kuiper belt objects. Most objects of the Kuiper belt (90%) have an inclination within 0.5 degrees. β is the ecliptic latitude.

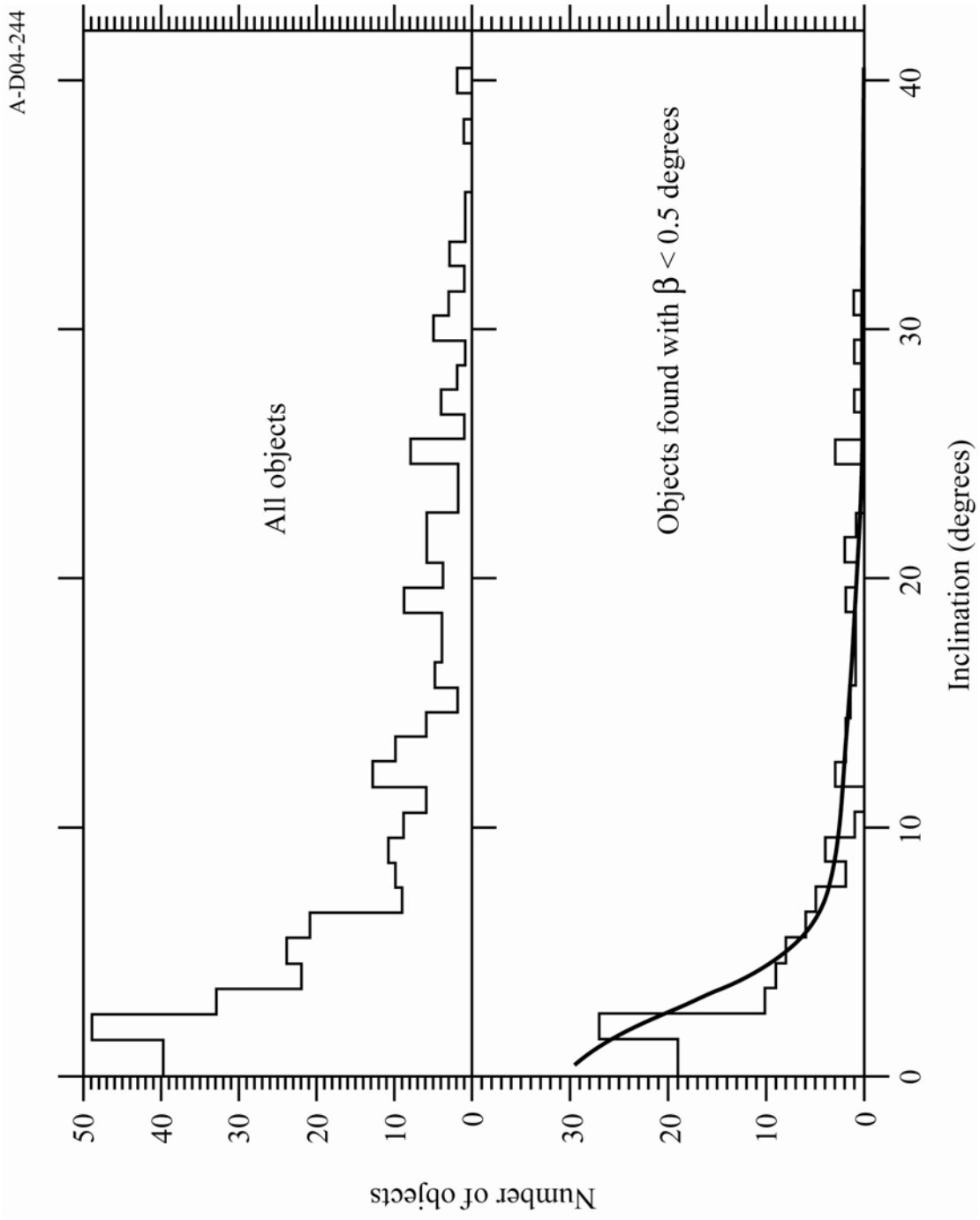
A-D04-244
All objects
Objects found with β < 0.5 degrees
Number of objects
Inclination (degrees)
0
10
20
30
40
50

Figure 11. The best-fit Poisson distribution ($N_m = N_0 e^{-\gamma \Delta t}$) of intervals between impacts. $N_0 = 43.05$ and $\gamma = 0.0302 \ \ s^{-1}$ for Voyager 2. The grey columns represent observed data and the line with spots shows Poisson fit.

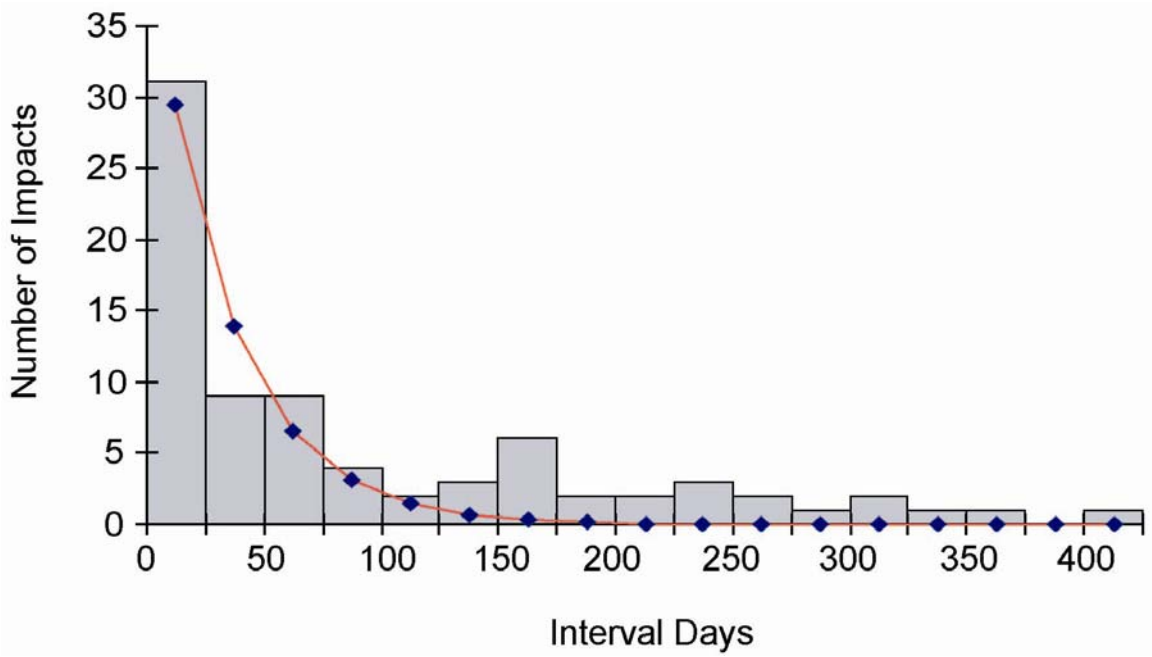
Number of Impacts
35
30
25
20
15
10
5
0
0
50
100
150
200
250
300
350
400
Interval Days

Figure 12. The best-fit Poisson distribution ($N_m = N_0 e^{-\gamma \Delta t}$) of intervals between impacts. $N_0 = 36.98$ and $\gamma = 0.0159\ s^{-1}$ for both Voyager 1 and Voyager 2. The grey columns represent observed data and the line with spots shows Poisson fit.

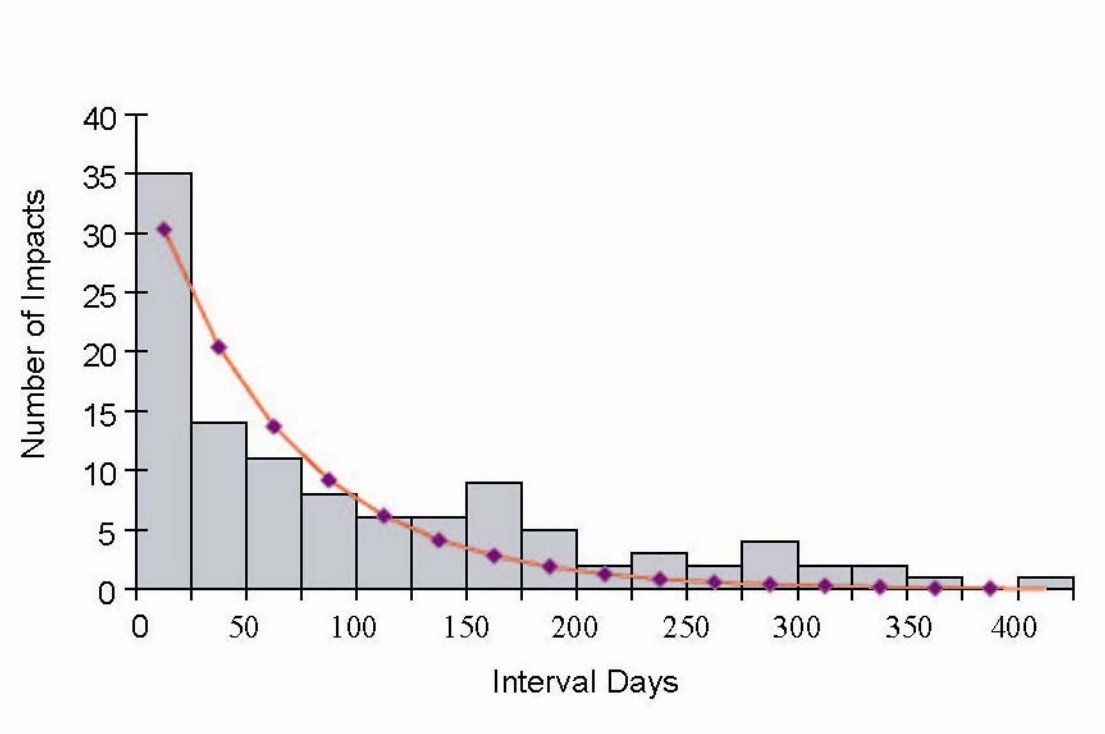
Number of Impacts
40
35
30
25
20
15
10
5
0
0
50
100
150
200
250
300
350
400
Interval Days

Figure 13. The best-fit Poisson distribution ($N_m = N_0 e^{-\gamma \Delta t}$) of intervals between impacts. $N_0 = 17.78$ and $\gamma = 0.0107\ s^{-1}$ for both Voyager 1 and Voyager 2 after 1986. The grey columns represent observed data and the line with spots shows Poisson fit.

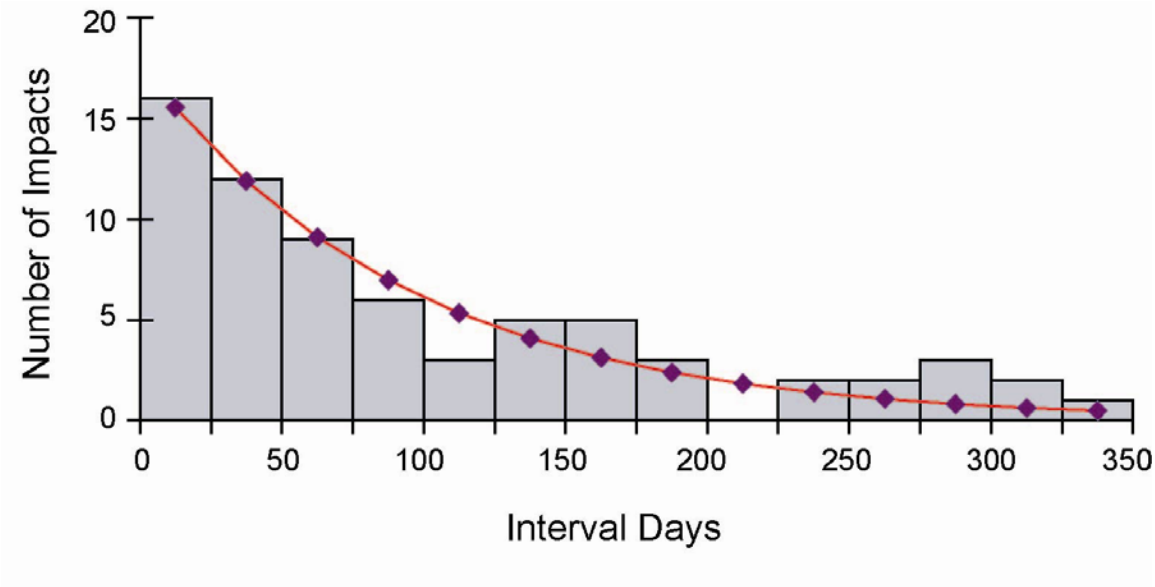
Number of Impacts
20
15
10
5
0
0
50
100
150
200
250
300
350
Interval Days

REFERENCES

Adams, N.G., and D. Smith (1971). Studies of microparticle impact phenomena leading to the development of a highly sensitive micrometeoroids detector. *Planet. Space Sci.* **19**, 195.

Auer, S., and K. Sitte (1968). Detection technique for micrometeoroids using impact ionization. *Earth Planet. Sci. Lett*. **4**, 178.

Brown, Michael E. (2001). The inclination distribution of the Kuiper belt. *The Astronomical Journal* **121**, 2804-2814.

Dietzel, H., G. Eichhorn, H. Fechtig, E. Grun, H.J. Hoffman, and J. Kissel (1973). The HEOS 2 and Helios micrometeoroid experiments. *J. Phys. E: Sci. Instrum*. **6**, 209.

Friichtenicht, J.F. (1964). Micrometeoroid simulation using nuclear acceleration techniques. *Nucl. Instrum. Methods* **28**, 70.

Grun, E. (1981). *Experimental Studies of Impact Ionization*. ESA Report (Paris) **SP-155**, 81.

Grun, E., H.A. Zook, M. Baguhl, A. Balogh, S.J. Bame, H. Fechtig, R. Forsyth, M.S. Hanner, M. Horanyi, J. Kissel, B.A. Lindblad, D. Linkert, G. Linkert, I. Mann, J.A. M. McDonnell, G.E. Morfill, J.L. Phillips, C. Polanskey, G. Schwehm, N. Siddique, P. Staubach, J. Svestka, and A. Taylor (1993). Discovery of Jovian dust streams and interstellar grains by the Ulysses spacecraft. *Nature* **362**, 428.

Gurnett, D.A., E. Grun, D.L. Gallagher, W.S. Kurth, and F.L. Scarf (1983). Micron-sized particles detected near Saturn by the Voyager plasma wave instrument. *Icarus*, **53**, 236-254.

Kruger, H., E. Grun, D.P. Hamilton, M. Baguhl, S. Dermott, H. Fechtig, B.A. Gustafsson, M.S. Hanner, M. Horanyi, J. Kissel, B.A. Lindblad, D. Linkert, G. Linkert, I. Mann, J.A.M. McDonnell, G.E. Morfill, C. Polanskey, R. Riemann, G. Schwehm, R. Srama, and H.A. Zook (1998). Three years of Galileo dust data. *Astro-Ph.* **V1**, 24.

Luu, J.X., and D.C. Jewitt (1996). The Kuiper belt. *Scientific American* **46**-52.

McDonnell, J.A.M. (1978). Microparticle studies by space instrumentation. In *Cosmic Dust* (J.A.M.McDonnell, ed.),. Wiley, New York.

Scarf, F.L., and D.A. Gurnett (1977). A plasma wave investigation for the Voyager mission. *Space Sci. Rev.* **21**, 289-308.